International Journal of Minerals, Metallurgy and Materials
Volume 25, Number 8, August 2018, Page 849
https://doi.org/10.1007/s12613-018-1634-3

Improved hemimorphite flotation using xanthate as a collector with S(II) and Pb(II) activation

Kai Jia, Qi-ming Feng, Guo-fan Zhang, Qing Shi, Yuan-jia Luo, and Chang-bin Li

School of Mineral Processing and Bioengineering, Central South University, Changsha 410083, China
(Received: 22 November 2017; revised: 22 December 2017; accepted: 26 December 2017)

Abstract: The flotation of hemimorphite using the S(II)–Pb(II)–xanthate process, which includes sulfidization with sodium sulfide, activation by lead cations, and subsequent flotation with xanthate, was investigated. The flotation results indicated that hemimorphite floats when the S(II)–Pb(II)–xanthate process is used; a maximum recovery of approximately 90% was obtained. Zeta-potential, contact-angle, scanning electron microscopy–energy-dispersive spectrometry (SEM–EDS), and diffuse-reflectance infrared Fourier transform spectroscopy (DRIFTS) measurements were used to characterize the activation products on the hemimorphite surface and their subsequent interaction with sodium butyl xanthate (SBX). The results showed that a ZnS coating formed on the hemimorphite surface after the sample was conditioned in an Na_2S solution. However, the formation of a ZnS coating on the hemimorphite surface did not improve hemimorphite flotation. With the subsequent addition of lead cations, PbS species formed on the mineral surface. The formation of the PbS species on the surface of hemimorphite significantly increased the adsorption capacity of SBX, forming lead xanthate (referred to as chemical adsorption) and leading to a substantial improvement in hemimorphite flotation. Our results indicate that the addition of lead cations is a critical step in the successful flotation of hemimorphite using the sulfidization–lead ion activation–xanthate process.

Keywords: hemimorphite; sulfidization; lead ion activation; xanthate; zeta potential; DRIFTS

1. Introduction

Zinc metal is the third most widely used nonferrous metal after copper and aluminum [1]. Currently, most of the world's zinc metal is produced from sulfide ore resources [2]. China holds 4.3×10^7 t of zinc metal reserves, and approximately 36wt% of these reserves are sourced from oxidized zinc ore resources (oxidation rate greater than 30wt%) [3]. For example, the Lanping lead zinc deposit, which may rank as the second largest in the world, contains 1.3×10^7 t of zinc metal; however, nearly 30wt% of the zinc ore is generally considered to be zinc oxide ore [4]. Undoubtedly, with the gradual exhaustion of the free-milling zinc sulfide ore resources and stricter SO_2 emissions standards, exploitation of this zinc oxide ore is becoming imperative [5].

Because of its high efficiency, low cost, and good adaptability, flotation is one of the most widely used techniques in mineral processing to achieve mineral separation [6]. The benefits of zinc sulfide ores can be easily realized through flotation with thiol collectors; however, concentrating zinc oxide ores by flotation is substantially more difficult [7–8]. Mining enterprises often only exploit the rich ores and discard the lean ores; the rich ores are then treated by direct hydrometallurgy without flotation. This process results in substantial waste of resources and considerable damage to the ecological environment surrounding the mining areas [9]. Therefore, developing an approach for exploiting zinc oxide ores using flotation has become an urgent issue in the zinc industry.

To date, several processes have been used for the flotation of zinc oxide ores [10]: sulfidization using a sulfurizing reagent and flotation using an amine collector; flotation using a fatty acid collector; flotation using a chelating collector. The most widely used technique in the flotation of zinc oxide ores is the sulfidization–amine collector method [11–12]. This route has poor performance for the flotation of hemimorphite because the amine collector is sensitive to slime. The slurry contains a large amount of slime, especially oxidized

Corresponding author: Guo-fan Zhang E-mail: zhangguofancsu01@126.com

ore slime, during the processing of hemimorphite ore, which results in poor flotation performance because of poor selectivity [11]. Fatty acid collectors show poor selectivity in the flotation of zinc oxide ores, especially when the hemimorphite ore contains gangues such as calcite or dolomite [13]. Chelate-forming collectors are organic molecules that contain at least two functional groups capable of bonding to the same metal atom [10]. However, because of the high cost of producing chelating collectors and the lack of a long-chain hydrophobic hydrocarbon in the molecules, chelating collectors have not been used in large-scale industrial applications [14].

The sulfidization–xanthate collector route has been successfully used in the industrial flotation of lead oxide ores and copper oxide ores [15–19], whose properties are highly similar to those of zinc oxide ores. Therefore, we assume that this route can be applied to the flotation of zinc oxide ores for industrial use. For this method, the most important step is the sulfurization procedure. The dose of the sulfiding agent, such as sodium sulfide (Na_2S), is critical to achieving successful flotation. Excess sulfiding agent strongly depresses flotation, whereas an insufficient amount does not adequately improve the floatability [18,20–21]. Current research on the sulfurization–xanthate process for the flotation of zinc oxide ores is mainly focused on the smithsonite minerals. Wu *et al.* [22], who have recently studied the interaction between Na_2S and smithsonite, demonstrated that the sulfidization product formed on the surface was ZnS. Unfortunately, for metal silicate minerals such as chrysocolla or hemimorphite, the sulfurization procedure is even more difficult [23].

Hemimorphite is a zinc hydroxyl silicate hydrate with the chemical formula $Zn_4(H_2O)[Si_2O_7](OH)_2$. Hemimorphite is the most abundant zinc oxide ore, second only to smithsonite, and it is mainly distributed in the United States, Mexico, Congo, Germany, Austria, and China [24]. Presently, research on the flotation of zinc oxide ore using the sulfidization–xanthate collector route is insufficient; in particular, the literature contains very few studies regarding the zinc silicate mineral hemimorphite. In the present study, the flotation of hemimorphite using the S(II)–Pb(II)–xanthate process, including sulfidization with Na_2S, activation by lead cations, and subsequent flotation with xanthate, was studied. We used a combination of zeta-potential, contact-angle, and scanning electron microscopy–energy-dispersive spectrometry (SEM–EDS) measurements to explore the activation mechanism involved in the S(II)–Pb(II)–xanthate process. Finally, the interactions between xanthate and fresh/activated hemimorphite minerals were investigated using diffuse-reflectance infrared Fourier transform spectroscopy (DRIFTS) to clarify the effects of hemimorphite activation on xanthate adsorption. Our findings could aid in the development of an ore flotation process for industrial use.

2. Experimental

2.1. Materials

A high-purity natural hemimorphite ($Zn_4(H_2O)[Si_2O_7](OH)_2$) sample (Yunnan province, China) was used in this study. The chemical composition of the sample was studied by X-ray fluorescence (XRF, Philips X Unique2); the results are shown in Table 1. The sharp and narrow peaks observed in the X-ray diffraction (XRD, Bruker D8 Advance powder diffractometer with Co K_α radiation source) pattern indicate that the hemimorphite sample was pure (Fig. 1). Some cubic pieces from the large specimens of hemimorphite were used for contact-angle measurements. The other samples were dry ground with a ceramic mortar and pestle and then screened with stainless steel sieves. The +38 to −106 μm size range was used in the microflotation tests, and the <38 μm size fraction was further ground in an agate mortar to obtain a particle size of <5 μm; this sample was subsequently used in the zeta-potential, SEM–EDS, and DRIFTS measurements.

Table 1. XRF chemical analysis of the fresh hemimorphite sample wt%

Zn	O	Si	P	Pb	S	Other
57.98	27.88	11.27	0.15	0.10	0.05	2.57

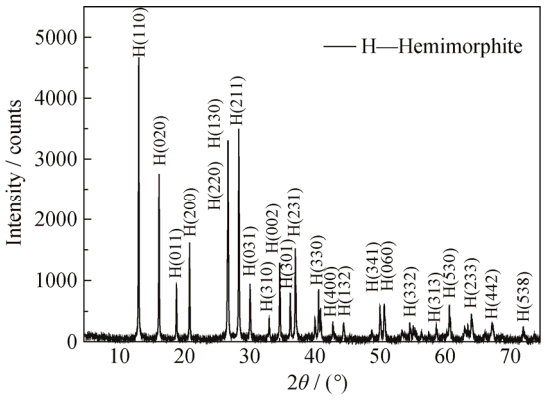

Fig. 1. X-ray diffraction pattern of the fresh hemimorphite sample.

Commercial-grade sodium butyl xanthate (SBX) (purchased from Honghua Reagent, Changsha, China), which was used as a collector, was purified by dissolution in acetone and recrystallization in petroleum ether. Methyl isobu-

tyl carbinol (MIBC) was used as a frother. The water used in this study was ultrapure water. Sodium sulfide (Na_2S) and lead nitrate ($Pb(NO_3)_2$) were used as the sulfiding agent and the metal-ion activator, respectively. Hydrochloric acid (HCl) and sodium hydroxide (NaOH) were used to adjust the pH value. A KNO_3 solution (2×10^{-3} M) was used to maintain the ionic strength. All tests were performed at room temperature (25°C), and unless otherwise stated, all chemicals used in this study were of analytical grade.

2.2. Methods

2.2.1. Microflotation

Flotation was achieved in an XFG flotation machine with a rotational speed of 1900 r/min. First, a 2.0 g sample of hemimorphite with particle sizes ranging from 38 to 106 μm was added to the flotation tank and 40 mL of ultrapure water was added. The samples were conditioned in ultrapure water for 3 min and then conditioned in the reagent levels as follows: SBX (3 min); Na_2S (3 min)–SBX (3 min), and Na_2S (3 min)–$Pb(NO_3)_2$ (3 min)–SBX (3 min). After the frother (MIBC) was added, the suspension was agitated for 1 min and the pH value was measured before flotation. The flotation was conducted for 5 min; the concentrate and tailings were then collected, dried, and weighed for calculation of the flotation recovery.

2.2.2. Zeta-potential measurements

Zeta-potential measurements of the hemimorphite particles conditioned with the given reagents were obtained using a Brookhaven zeta-potential analyzer. In each case, the test was conducted in a 2×10^{-3} M KNO_3 background electrolyte solution. A 0.03 g sample of hemimorphite was dispersed in 80 mL of electrolyte solution for 5 min, and the pH value of the resultant suspension was adjusted. Next, a few milliliters of the dispersion from the top of the suspension was transferred by syringe into the electrophoretic cell and the zeta potential was measured. Three tests were conducted for each measurement, and the results were subsequently averaged.

For the experiments of sulfurized hemimorphite samples, the ultrasound-treated samples were conditioned in a 1×10^{-3} M Na_2S solution for 10 min. The sulfurized samples were then cleaned to eliminate the residual S(II) and any suspended colloidal particles on the mineral surface through a centrifugation/decantation and washing stage. After the samples were conditioned with pH modifier, the zeta-potential measurements were conducted as previously described. The experiments were repeated for the hemimorphite samples treated with Na_2S (1×10^{-3} M, 10 min)–$Pb(NO_3)_2$ (1×10^{-3} M, 10 min) and Na_2S (1×10^{-3} M, 10 min)–$Pb(NO_3)_2$ (1×10^{-3} M, 10 min)–SBX (2×10^{-3} M, 5 min).

2.2.3. Contact-angle measurements

The contact angle was measured using a DIGIDROP-DS goniometer (GBX, France) via the sessile-drop method. The cut, hand-picked, and pure crystalline hemimorphite samples were successively polished with 6, 3, and 0.5 μm liquid diamond paste on the polishing cloth and then cleaned with ultrapure water. The samples were prepared following the same procedure as that used for the zeta-potential experiments. After conditioning, the polished minerals were washed twice with ultrapure water, dried in a vacuum drying oven at 20°C, and then used for contact-angle measurements. Each sample was placed on the stage with its polished face pointing upward. A 4 μL droplet of ultrapure water was deposited onto the polished face of the sample, and the contact angle was simultaneously measured. The contact angle was automatically calculated by the GBX software. The contact angles of five different areas of each sample were measured, and the values were averaged [25].

2.2.4. SEM–EDS observations

The samples used for SEM measurements were conditioned using the same procedure as that used for the contact-angle measurements. A KYKY-2800 scanning electron microscope was used to observe the samples. Chemical analysis of the new film formed on the hemimorphite surface was conducted using a FINDER-1000 energy-dispersive spectrometer. The samples were coated with a thin layer of gold to prevent charging [26].

2.2.5. DRIFTS measurements

DRIFTS measurements were performed using a Shimadzu IRAffinity-1 Fourier transform infrared (FTIR) spectrophotometer (Shimadzu, Japan) equipped with a Shimadzu sampling accessory (DRS8000A) operating in diffuse-reflection mode. The samples were conditioned using the same procedure as that used for the contact-angle measurements, except that the concentration of SBX was 0.2 M in each test. Each sample was transferred onto a DRIFTS sample holder and flattened with a plastic coverslip. Each spectrum was recorded at a resolution of 4 cm^{-1} in the 4000–400 cm^{-1} region after 100 scans against a KBr background.

3. Results and discussion

3.1. Flotation performance of hemimorphite

Fig. 2 shows hemimorphite flotation as a function of the lead ion concentration in the presence of increasing concentrations of Na_2S. In the absence of either Na_2S or lead ions, hemimorphite displayed very poor floatability when SBX

was used as a collector, with a maximum recovery of only 33% (point 1, Fig. 2). However, as shown in Fig. 2 (point 2), the sulfidization process did not substantially improve the flotation of hemimorphite. Instead, the addition of Na_2S resulted in a substantial decrease in hemimorphite flotation. However, regardless of whether a ZnS species was formed at the mineral surface after sulfidization conditioning, the unexpected abundance of residual sulfur ions in the pulp depressed flotation [27–29]. The depression of sulfidized hemimorphite was analogous to the mechanism of sphalerite depression by S(II) when thio-compounds were used as collectors. The addition of Pb(II) yielded a significant improvement in hemimorphite flotation, and a maximum recovery of 90% was obtained (point 3, Fig. 2). The relationship between the Na_2S and Pb(II) concentrations exerted an obvious effect on hemimorphite flotation, and the maximum recovery occurred when the [S(II)]/[Pb(II)] ratio was approximately 1 in solution. Our results indicate that the S(II)–Pb(II)–xanthate process can successfully induce flotation of the refractory hemimorphite and that the addition of Pb(II) is essential for this sulfidization–xanthate technology.

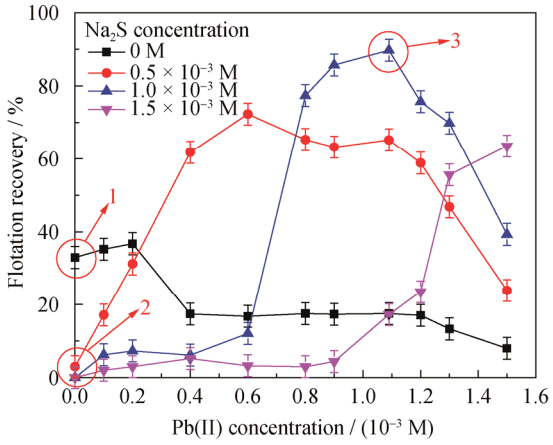

Fig. 2. Effects of the Na_2S and Pb(II) concentrations on the flotation behavior of hemimorphite at 2 × 10^{-3} M SBX (at a pH value of approximately 9).

3.2. Zeta-potential analysis

Zeta-potential measurements were used to study the adsorption of additives onto the surfaces of hemimorphite samples involved in the S(II)–Pb(II)–SBX process because the shift in the zeta potential of the corresponding conditioned sample indicates whether the SH^-, Pb(II), or SBX from the solution was adsorbed onto the mineral surface [30–31]. Fig. 3 shows the zeta potential of hemimorphite as a function of pH value before and after activation in the presence and absence of a collector. As shown in curves a and b in Fig. 3, the presence of Na_2S caused the zeta potential of the minerals to shift in the negative direction. This change is attributed to the adsorption of S^{2-} or SH^- from the solution.

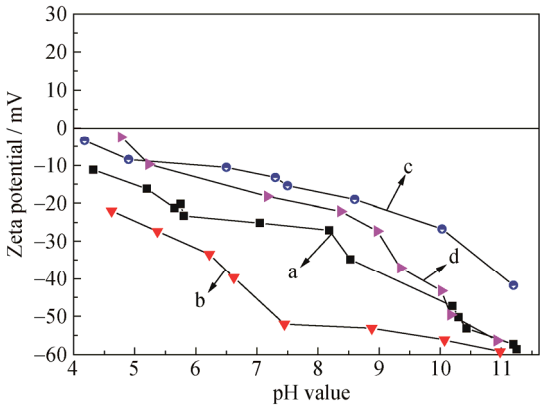

Fig. 3. Zeta potential of hemimorphite as a function of pH value: (a) fresh hemimorphite; (b) He + 1 × 10^{-3} M Na_2S (decantation); (c) He + 1 × 10^{-3} M Na_2S (decantation) + 1 × 10^{-3} M Pb(II) (decantation); (d) He + 1 × 10^{-3} M Na_2S (decantation) + 1 × 10^{-3} M Pb(II) (decantation) + 2 × 10^{-3} M SBX. "He" denotes hemimorphite.

The zeta potential of the sulfurized hemimorphite activated by Pb(II) (labelled as sample c) as a function of pH is shown in curve c in Fig. 3. The increased zeta-potential value of sample c indicates that the Pb(II) from the solution adsorbed onto the surface of the mineral sample [32]. Furthermore, the results show that the color of the mineral samples gradually deepened from dark-yellow to dark-black with the addition of Pb(II).

After pretreatment with the S(II)–Pb(II) process, the hemimorphite samples were conditioned in an SBX solution (labelled as sample d). The zeta potential of sample d shifted in the negative direction compared with that of sample c, indicating butyl xanthate anions (BX^-) adsorbed onto the hemimorphite surface pre-modified by Na_2S and Pb(II).

3.3. Contact-angle measurements

Changes in the contact angle of the mineral surface before and after treatment with reagents can be used to indirectly show the change in hydrophobicity of the mineral and to characterize the reagent adsorption mechanism on the mineral surface [33–34].

As shown in Fig. 4, the contact angle of fresh hemimorphite is 22.66°, and the sample exhibits high hydrophilicity and poor floatability [35–36]. After the hemimorphite sample was conditioned in SBX solution, its contact angle increased to 53.51° because of slight SBX adsorption. The contact angle of sample 3 (hemimorphite + Na_2S + SBX) further increased to 64.38°. Sample 4 (hemimorphite + Na_2S + Pb(II) + SBX) exhibited the highest contact angle of

93.60°, with the corresponding highest hydrophobicity and floatability, which suggests that the surface of sample 4 had the strongest affinity toward the collector, resulting in this sample exhibiting the highest adsorption level of SBX among the investigated samples [37]. This result was most likely due to the formation of PbS species, which occurs as a result of Pb(II) activation on the surface. This phenomenon is similar to that of natural galena, which has the highest adsorption capacity of xanthate.

3.4. SEM and EDS analyses

We observed the hemimorphite samples by SEM to analyze the morphology of fresh hemimorphite (Fig. 5(a)) and hemimorphite conditioned in an Na_2S solution (Fig. 5(b)) or with the S(II)–Pb(II) process (Fig. 5(c)). The hemimorphite samples before and after conditioning in an Na_2S solution exhibited a smooth surface (Figs. 5(a) and 5(b)), whereas the hemimorphite conditioned in an Na_2S solution followed by Pb(II) activation exhibited a rough surface and contained numerous fine floccules of compounds with a diameter of approximately 30–50 nm (Fig. 5(c)). The flocculent shape of the mineral surface might be derived from the crystal structure of the newly formed compounds.

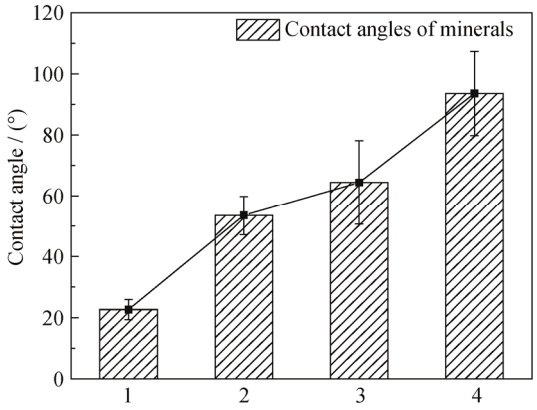

Fig. 4. Comparison of the contact angles of the samples: 1—fresh hemimorphite; 2—He + 2 × 10^{-3} M SBX; 3—He + 1 × 10^{-3} M Na_2S (decantation) + 2 × 10^{-3} M SBX; 4—He + 1 × 10^{-3} M Na_2S (decantation) + 1 × 10^{-3} M Pb(II) (decantation) + 2 × 10^{-3} M SBX. "He" denotes hemimorphite.

Fig. 6 shows the EDS results of the corresponding mineral samples. Sulfur peaks were not observed for the fresh hemimorphite samples (Fig. 6(a)), consistent with the XRF results (Table 1). To ensure the accuracy of the results, we selected two locations representing coarse and fine particles for analysis of the surface elemental contents of the conditioned samples (b and c).

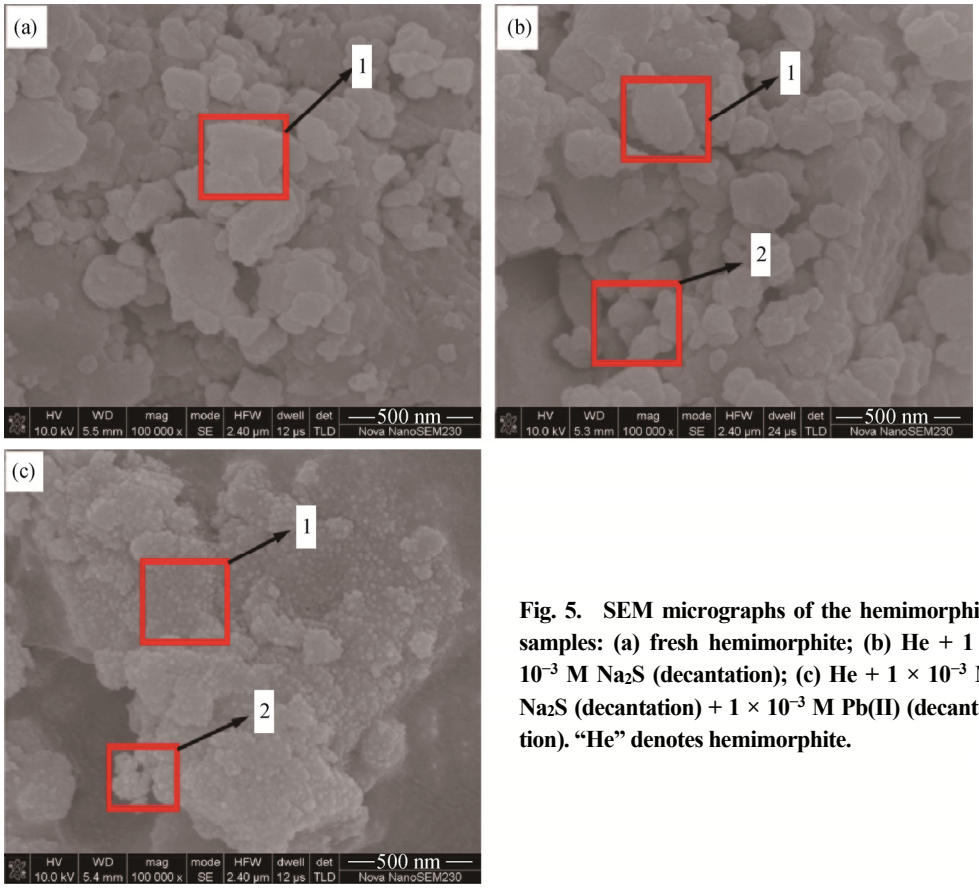

Fig. 5. SEM micrographs of the hemimorphite samples: (a) fresh hemimorphite; (b) He + 1 × 10^{-3} M Na_2S (decantation); (c) He + 1 × 10^{-3} M Na_2S (decantation) + 1 × 10^{-3} M Pb(II) (decantation). "He" denotes hemimorphite.

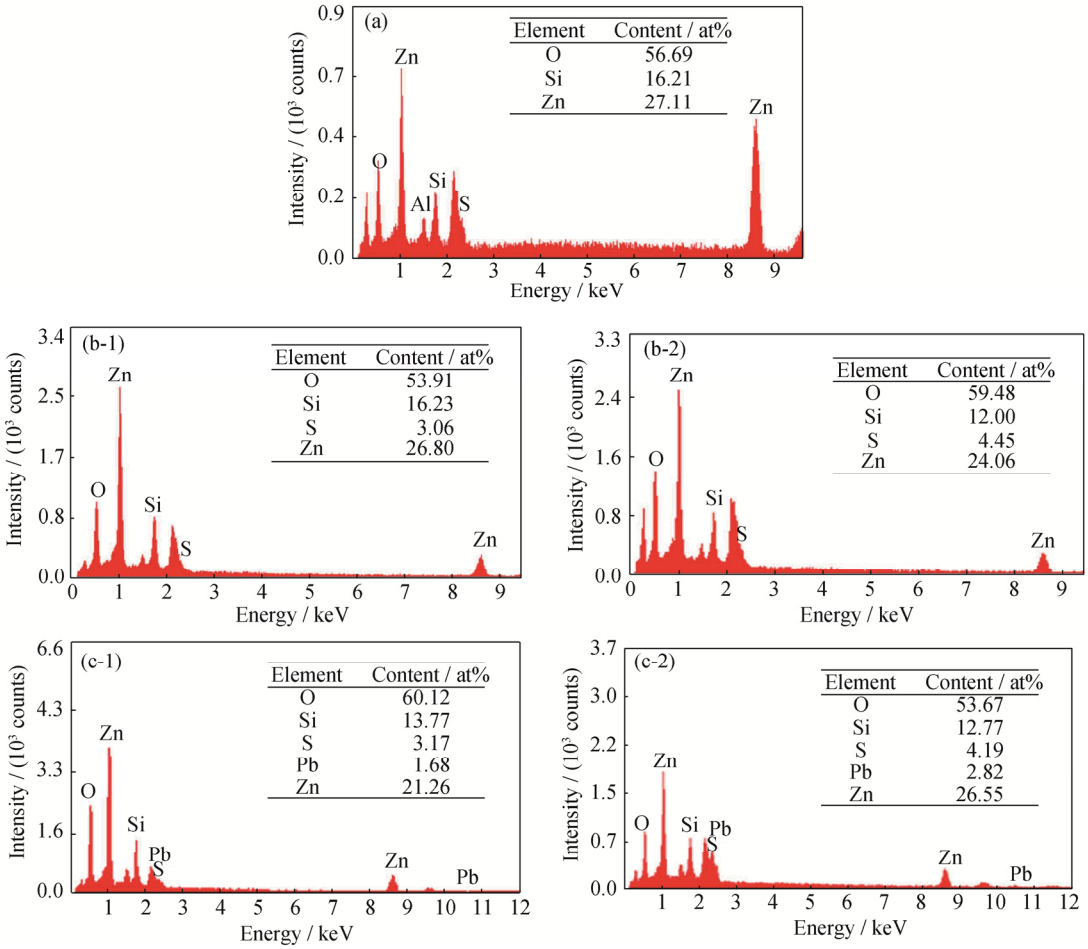

Fig. 6. EDS spectra collected from the rectangular zones of Fig. 5: (a) point 1 marked in Fig. 5(a); (b-1) point 1 marked in Fig. 5(b); (b-2) point 2 marked in Fig. 5(b); (c-1) point 1 marked in Fig. 5(c); (c-2) point 2 marked in Fig. 5(c).

For the sulfurized sample, the EDS spectrum shows an S peak as well as peaks that correspond to hemimorphite (Zn, O, Si). More sulfur atoms adsorbed onto the fine particles (area 2 in Fig. 5(b)) than onto the coarse particles (area 1 in Fig. 5(b)), likely because of the large specific area and the resulting high activity of the fine particles. Because the centrifugation/decantation and washing procedures eliminated the interference from the residual sulfur ions in solution, this observation provides conclusive evidence for the existence of a sulfide film.

The EDS results of sample c are shown in Fig. 6, which shows that, in addition to the peaks of Zn, O, and Si corresponding to hemimorphite, the presence of Pb and S peaks indicates that PbS-like species formed on the surface and that the fine slime (area 2 in Fig. 5(c)) particles contained more Pb and S than the coarse slime (area 1 in Fig. 5(c)) particles. The fine floccules of compounds on sample c, as revealed by the SEM images, are most likely crystalline PbS. Because the sulfurized hemimorphite was rinsed thoroughly to remove the remaining S(II) from the solution, all of the newly formed PbS species at the surface were PbS grains derived from the interactions of Pb(II) with sulfur atoms from newly generated ZnS species and were not derived from precipitation reactions. However, the semi-quantitative results of S from the surface are not accurate because the peaks of S overlap with those of Au (a gold coating was used for SEM–EDS) and the atomic ratio of Pb/S could not be used to characterize the stoichiometric composition of the newly generated species [36]. Our results confirmed the presence of PbS species at the conditioned hemimorphite surface.

3.5. DRIFTS spectral analysis

To better understand the adsorption mechanism of SBX by hemimorphite samples before and after conditioning, DRIFTS was performed. Fig. 7 shows the DRIFTS spectra of the hemimorphite pretreated with S^{2-} or Pb(II) with and without SBX.

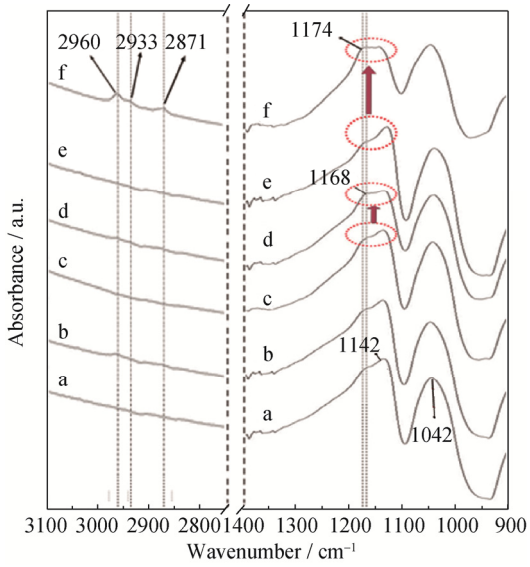

Fig. 7. DRIFTS spectra of the hemimorphite samples: (a) fresh hemimorphite; (b) He + 0.2 M SBX; (c) He + 1 × 10^{-3} M Na_2S (decantation); (d) He + 1 × 10^{-3} M Na_2S (decantation) + 0.2 M SBX; (e) He + 1 × 10^{-3} M Na_2S (decantation) + 1 × 10^{-3} M Pb(II) (decantation); and (f) He + 1 × 10^{-3} M Na_2S (decantation) + 1 × 10^{-3} M Pb(II) (decantation) + 0.2 M SBX. "He" denotes hemimorphite.

The two broad intense bands located at approximately 1042 and 1142 cm^{-1} in the spectra in Fig. 7 are attributed to the Si–O_{nb} vibration and ν_{as}(Si–O_b–Si) vibration in hemimorphite, respectively [38–39]. Curves a and b in Fig. 7 shows that the infrared spectra of hemimorphite before and after immersion in 0.2 M SBX without sulfidization are basically the same and that no absorption peaks attributable to xanthate species are observed. Curves c and d in Fig. 7 shows the spectra of the presulfurized hemimorphite before and after interaction with SBX (0.2 M). Because of overlap between the weak peaks of adsorbed butylxanthate species and the intense peaks of hemimorphite in the region from 1300 to 900 cm^{-1}, where some characteristic vibrations of the xanthate functional groups occur [40–41], useful chemical information about the adsorbate is difficult to discern in this region. Only a new weak band at 1168 cm^{-1} was observed in curve d. Curves e and f in Fig. 7 shows the spectra of presulfurized hemimorphite with subsequent activation by Pb(II) before and after interaction with SBX (0.2 M). In this case, a new weak band is observed at 1174 cm^{-1} in curve f.

The new bands at 1168 and 1174 cm^{-1} are characteristic of zinc xanthate ($Zn(BX)_2$) and lead xanthate ($Pb(BX)_2$) coordination complexes, respectively, and can be assigned to C–O–C asymmetric stretching [42–46]. This result indicates that the chemisorbed metal xanthate ($Me(BX)_2$) coordination complex was formed on the surface of the sulfurized hemimorphite. Interestingly, new intense peaks located at 2871, 2933, and 2960 cm^{-1} were observed only for the hemimorphite sample treated with the S(II)–Pb(II)-SBX process in curve f. According to previous studies [47–50], the band at 2871 cm^{-1} is associated with symmetric CH_3 stretching vibrations, the band at 2933 cm^{-1} is assigned to asymmetric CH_2 stretching, and the band at 2960 cm^{-1} is due to asymmetric CH_3 stretching. These new intense bands are associated with molecules containing long alkyl chains that originated from adsorbed SBX species at the surface, indicating that the newly formed PbS on the surface of the sample treated with the S(II)–Pb(II) process has a much stronger affinity for xanthate than the corresponding ZnS species on the surface of the sample treated with S(II), which improves the flotation of hemimorphite.

3.6. Mechanism

Hemimorphite is a sorosilicate silicate mineral composed of Si_2O_7 units. As shown in Fig. 8, the crystal structure of hemimorphite includes zinc atoms coordinated with three oxygen atoms of an Si_2O_7 group and one oxygen atom of a hydroxide ion to form a Zn–O tetrahedron. The Si_2O_7 group is composed of two Si–O tetrahedra linked by a common oxygen atom. Both crystal water (a in Fig. 8) and frame water (b in Fig. 8) exist in the structures of hemimorphite minerals [39,51].

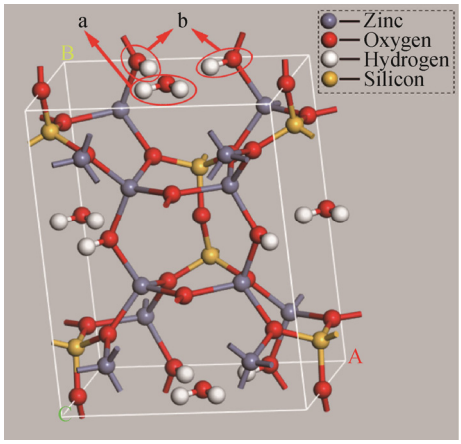

Fig. 8. A 3-dimensional view of the bulk lattice structure of hemimorphite.

Because the frame water molecules are arranged on the (110) surface of the hemimorphite crystal, perfect cleavage occurs along the (110) plane. The Zn–O bonds are broken along the (110) plane by fracture or cleavage, and the Zn atom of the Zn–O tetrahedron and the OH^- in the crystal skeleton are exposed on the (110) cleavage surface, as shown in Fig. 9 [52].

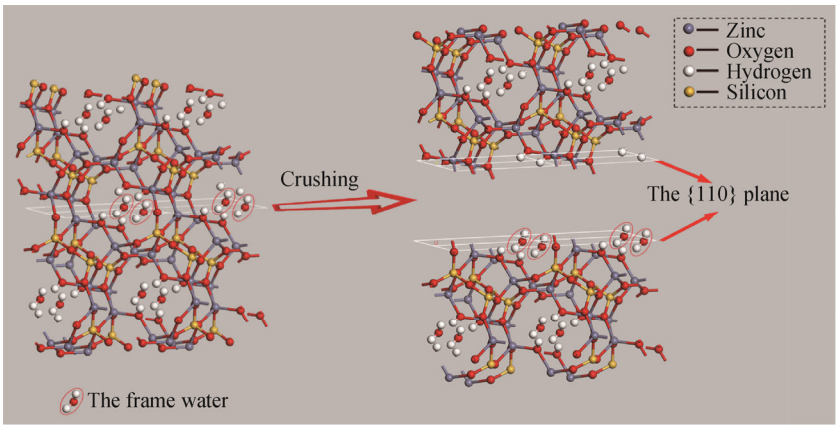

Fig. 9. Schematic of the cleavage of hemimorphite along the (110) plane.

According to the theory of chemical reaction kinetics, the reason for the solid–liquid interface reaction when a solid is immersed into a liquid arises from the collision of the reactants in the solution with the solid reactants. In a heterogeneous reaction, collision and reaction occur after the adsorption of the reactants onto the solid surface. The solid–liquid reaction process of hemimorphite in aqueous solution can be decomposed into several processes. First, the water molecules adsorb onto the cleavage surface of hemimorphite, and a hydration film is formed. The exposed Zn atoms react quickly with the OH^- ions, forming zinc oxyhydroxide, as suggested in Fig. 10. Because the hydroxylation products on the surface are hydrophilic, natural hemimorphite has a strong affinity for water, with a contact angle of 22.66° (sample 1, Fig. 4) [53].

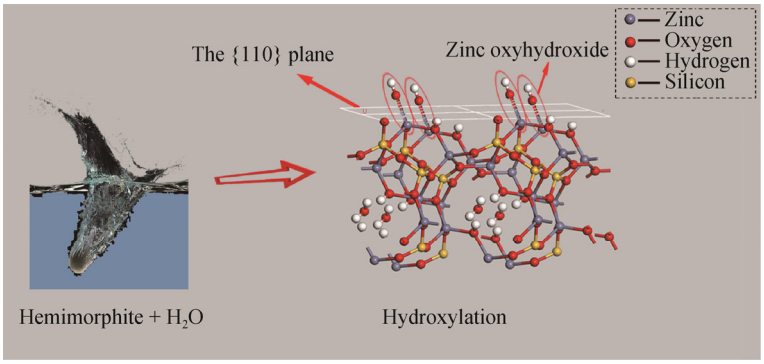

Fig. 10. Schematic of the hydroxylation of exposed zinc atoms on the (110) surface of hemimorphite (the dotted lines represent the metal–hydroxyl coordination bonds).

The flotation results show that hemimorphite can be successfully floated using the S(II)–Pb(II)–SBX process. According to the negative shift in the zeta potential after conditioning in an Na_2S solution, the S^{2-} or SH^- ions were adsorbed onto the hemimorphite surface. A film of ZnS-like species was formed on the surface, which was further confirmed by the contact-angle and SEM–EDS results. Notably, the contact-angle and SEM–EDS results did not contradict the flotation result for sulfurized hemimorphite (point 2, Fig. 2) because residual sulfur ions were present in the flotation pulp. This new film was similar to natural sphalerite, including the very apparent color change from white to canary yellow. At a pH value of approximately 9, where the highest flotation recovery was obtained, the sulfidization of hemimorphite by Na_2S occurred by forming more insoluble ZnS compounds, as shown in Fig. 11.

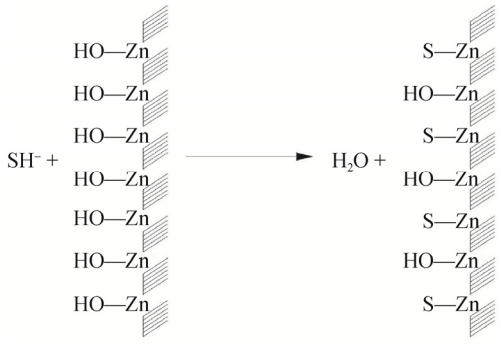

Fig. 11. Schematic of sulfurized interactions that may occur at the hemimorphite surface (at pH 9).

Sphalerite responds poorly to xanthate collectors compared with other metal sulfide minerals (e.g., galena and chalcocite), largely because of the good solubility of Zn–xanthate species [54–58]. In addition, the newly formed quasi-sphalerite film on the hemimorphite surface was very thin. As a result, the sulfurized hemimorphite exhibited a weak affinity for SBX, as demonstrated by the contact-angle measurement results (Fig. 4) and the DRIFTS results (Fig. 7). Additionally, the residual sulfur ions could strongly depress flotation, thus explaining why poor flotation was observed (Fig. 2).

Metal sulfide minerals are well known to be activated by heavy-metal ions such as Cu(II) and Pb(II) [59–60]. In this study, Pb(II) was chosen as the activator to further improve the flotation behavior of the sulfurized hemimorphite. With the subsequent addition of $Pb(NO_3)_2$, a layer of PbS-like species was formed on the hemimorphite surface, as demonstrated by the dramatic color change to bright black, the good flotation performance (Fig. 2), the contact-angle measurement results (Fig. 4), and the SEM–EDS results (Figs. 5 and 6).

The heavy-metal-ion activation process of sulfide minerals (equivalent to the newly formed ZnS-like species in this paper) is widely accepted as occurring via a substitution reaction. According to this hypothesis, the zinc atoms from the ZnS-like species newly generated on the hemimorphite surface were replaced by Pb(II) from the solution. This replacement could have resulted from the greater affinity of lead than zinc ions for sulfide ions. Additionally, the newly formed ZnS-like species exhibited higher chemical reactivity than natural sphalerite, which facilitated the substitution reaction, as shown in Fig. 12.

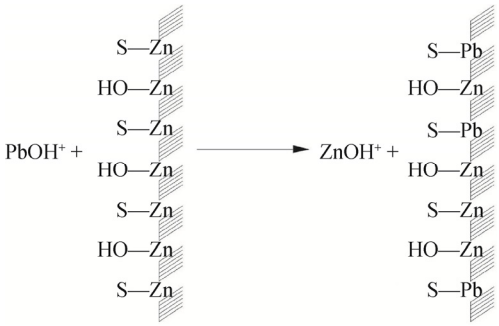

Fig. 12. Schematic of lead activation interactions that can occur at the Na_2S-conditioned hemimorphite surface (at pH 9).

These findings demonstrate that, with the addition of Pb(II) ions to the sulfurized hemimorphite pulp, the adsorption of the collector increased as a result of the formation of PbS on the surface of hemimorphite, as shown in the DRIFTS results (Fig. 7). The formation of $Pb(BX)_2$ indicates a strong chemical adsorption of xanthate onto the active sites of the hemimorphite surface. The increase in SBX adsorption resulted in a marked improvement in the final hemimorphite flotation. Thus, we can schematically represent the processes occurring at the hemimorphite–water interface in the S(II)–Pb(II)–SBX process, as shown in Fig. 13.

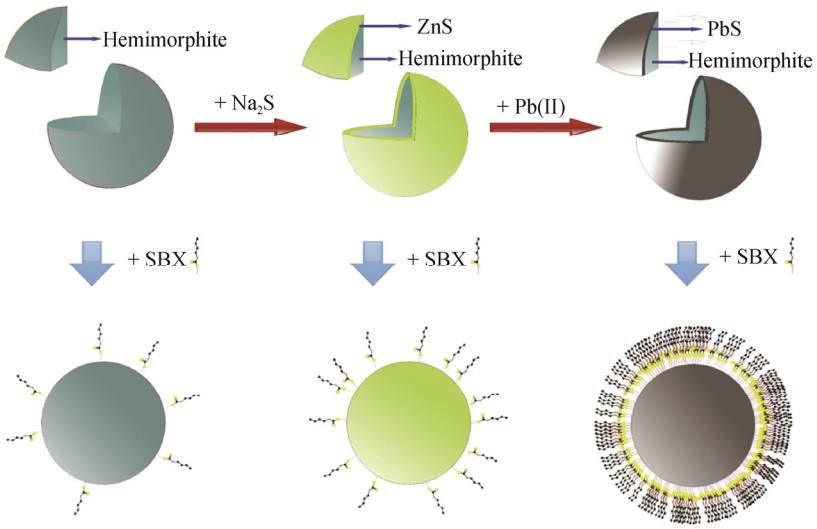

Fig. 13. Adsorption of SBX onto an activated or inactivated hemimorphite surface.

4. Conclusions

Our work examined hemimorphite flotation using the S(II)–Pb(II)–xanthate process. The surface chemistry involved in this process was investigated in detail via zeta-potential, contact-angle, SEM–EDS, and DRIFTS measurements to elucidate the mechanism of the activated reaction. On the basis of our results and discussion, the

principal outcomes are summarized as follows.

(1) The S(II)–Pb(II)–xanthate process, including sulfidization using sodium sulfide, activation by lead cations, and subsequent flotation with SBX, can successfully float hemimorphite, with a maximum recovery of approximately 90%.

(2) During the sulfidization process, the S^{2-} or SH^- ions adsorbed onto hemimorphite surfaces, and a film of ZnS-like species formed at the mineral surface. The newly formed ZnS-like film on the hemimorphite surface had a weak affinity for SBX; therefore, adsorption of SBX at the mineral surface was poor, as indicated by the DRIFTS experiments.

(3) The addition of lead ions induced a phase conversion at the sulfurized hemimorphite surface, and PbS coatings were formed. The newly formed PbS species exhibited a high adsorption capacity for xanthate, and high levels of SBX were chemisorbed onto the hemimorphite surface with the generation of $Pb(BX)_2$ (representing chemical adsorption), as determined by DRIFTS analysis. The resultant $Pb(BX)_2$ species significantly increased hemimorphite flotation.

Acknowledgements

This work was financially supported by the State Key Development Program for Basic Research of China (No. 2014CB643402) and the Collaborative Innovation Center for Clean and Efficient Utilization of Strategic Metal Mineral Resources of Central South University. We are grateful to Dr. Wen-cai Zhang of University of Kentucky for his comments on the manuscript. The authors also wish to thank Dr. Peng-fei Tan of Central South University for his assistance with the SEM and EDS experiments.

References

[1] N. Sorour, W. Zhang, G. Gabra, E. Ghali, and G. Houlachi, Electrochemical studies of ionic liquid additives during the zinc electrowinning process, *Hydrometallurgy*, 157(2015), p. 261.

[2] H.B. Zhao, X.W. Gan, J. Wang, L. Tao, W.Q. Qin, and G.Z. Qiu, Stepwise bioleaching of Cu-Zn mixed ores with comprehensive utilization of silver-bearing solid waste through a new technique process, *Hydrometallurgy*, 171(2017), p. 374.

[3] Q.M. Feng and G.F. Zhang, Original pulp flotation technology of the oxidized ore of zinc and lead(in Chinese), *China Basic Sci.*,(2011), No. 1, p. 25.

[4] T.L. Rao, Basical characteristics of lead-zinc mineral resources and the vista on geological prospecteing of super large scale lead-zinc deposits in Yunnan, *China Min. Mag.*, 17(2008), No. 3, p. 107.

[5] H.M. Shao, X.Y. Shen, Y. Sun, Y. Liu, and Y.C. Zhai, Reaction condition optimization and kinetic investigation of roasting zinc oxide ore using $(NH_4)_2SO_4$, *Int. J. Miner. Metall. Mater.*, 23(2016), No. 10, p. 1133.

[6] G. Kim, K. Park, J. Choi, A. Gomez-Flores, Y. Han, S.Q. Choi, and H. Kim, Bioflotation of malachite using different growth phases of Rhodococcus opacus: Effect of bacterial shape on detachment by shear flow, *Int. J. Miner. Process.*, 143(2015), p. 98.

[7] S.H. Hosseini and E. Forssberg, Physicochemical studies of smithsonite flotation using mixed anionic/cationic collector, *Miner. Eng.*, 20(2007), No. 6, p. 621.

[8] Y. Sun, X.Y. Shen, and Y.C. Zhai, Thermodynamics and kinetics of extracting zinc from zinc oxide ore by the ammonium sulfate roasting method, *Int. J. Miner. Metall. Mater.*, 22(2015), No. 5, p. 467.

[9] J. Wang, Q.W. Zhang, and F. Saito, Improvement in the floatability of CuO by dry grinding with sulphur, *Colloids Surf. A*, 302(2007), No. 1–3, p. 494.

[10] M. Irannajad, M. Ejtemaei, and M. Gharabaghi, The effect of reagents on selective flotation of smithsonite–calcite–quartz, *Miner. Eng.*, 22(2009), No. 9-10, p. 766.

[11] M. Ejtemaei, M. Irannajad, and M. Gharabaghi, Influence of important factors on flotation of zinc oxide mineral using cationic, anionic and mixed (cationic/anionic) collectors, *Miner. Eng.*, 24(2011), No. 13, p. 1402.

[12] A.L. Chen, M.C. Li, Z. Qian, Y.T. Ma, J.Y. Che, and Y.L. Ma, Hemimorphite ores: A review of processing technologies for zinc extraction, *JOM*, 68(2016), No. 10, p. 2688.

[13] H. Bustamante and H.L. Shergold, Surface chemistry and flotation of zinc oxide minerals: II.--Flotation with chelating reagents, *Trans. Inst. Min. Metall. Sect. C*, 92(1983), p. C208.

[14] A. Marabini, M. Ciriachi, P. Plescia, and M. Barbaro, Chelating reagents for flotation, *Miner. Eng.*, 20(2007), No. 10, p. 1014.

[15] R. Herrera-Urbina, F.J. Sotillo, and D.W. Fuerstenau, Effect of sodium sulfide additions on the pulp potential and amyl xanthate flotation of cerussite and galena, *Int. J. Miner. Process.*, 55(1999), No. 3, p. 157.

[16] Q.C. Feng, S.M. Wen, J.S. Deng, and W.J. Zhao, Combined DFT and XPS investigation of enhanced adsorption of sulfide species onto cerussite by surface modification with chloride, *Appl. Surf. Sci.*, 425(2017), p. 8.

[17] S. Castro, J. Goldfarb, and J. Laskowski, Sulphidizing reactions in the flotation of oxidized copper minerals, I. Chemical factors in the sulphidization of copper oxide, *Int. J. Miner. Process.*, 1(1974), No. 2, p. 141.

[18] K. Park, S. Park, J. Choi, G. Kim, M. Tong, and H. Kim, Influence of excess sulfide ions on the malachite-bubble interaction in the presence of thiol-collector, *Sep. Purif. Technol.*, 168(2016), p. 1.

[19] Z. Li, M. Chen, X.W. Li, Z.W. Lei, J. Qu, P.W. Huang, Q.W. Zhang, and F. Saito, Surface modification of basic copper

carbonate by mechanochemical processing with sulfur and ammonium sulfate, *Adv. Powder Technol.*, 28(2017), No. 8, p. 1877.

[20] K. Lee, D. Archibald, J. McLean, and M. Reuter, Flotation of mixed copper oxide and sulphide minerals with xanthate and hydroxamate collectors, *Miner. Eng.*, 22(2009), No. 4, p. 395.

[21] Q.C. Feng, S.M. Wen, W.J. Zhao, Q.B. Cao, and C. Lü, A novel method for improving cerussite sulfidization, *Int. J. Miner. Metall. Mater.*, 23(2016), No. 6, p. 609.

[22] D.D. Wu, S.M. Wen, J.S. Deng, J. Liu, and Y.B. Mao, Study on the sulfidation behavior of smithsonite, *Appl. Surf. Sci.*, 329(2015),p. 315.

[23] S. Raghavan, E. Adamec, and L. Lee, Sulfidization and flotation of chrysocolla and brochantite, *Int. J. Miner. Process.*, 12(1984), No. 1-3, p. 173.

[24] J.A. Ober, *Mineral Commodity Summaries 2016*, U.S. Geological Survey, Reston, Virginia, 2016.

[25] Y.H. Hu, Z.Y. Gao, W. Sun, and X.W. Liu, Anisotropic surface energies and adsorption behaviors of scheelite crystal, *Colloids Surf. A*, 415(2012), p. 439.

[26] S.C. Chelgani, B. Hart, J. Marois, and M. Ourriban, Study of pyrochlore matrix composition effects on froth flotation by SEM–EDX, *Miner. Eng.*, 30(2012), p. 62.

[27] R. Herrera-Urbina, F.J. Sotillo, and D.W. Fuerstenau, Amyl xanthate uptake by natural and sulfide-treated cerussite and galena, *Int. J. Miner. Process.*, 55(1998), No. 2, p. 113.

[28] M. Barbaro, R.H. Urbina, C. Cozza, D. Fuerstenau, and A. Marabini, Flotation of oxidized minerals of copper using a new synthetic chelating reagent as collector, *Int. J. Miner. Process.*, 50(1997), No. 4, p. 275.

[29] J.C.D. Gush, Flotation of oxide minerals by sulphidization-the development of a sulphidization control system for laboratory testwork, *J. South Afr. Inst. Min. Metall.*, 105(2005), No.3, p. 193.

[30] W. Nyabeze and B. McFadzean, Adsorption of copper sulphate on PGM-bearing ores and its influence on froth stability and flotation kinetics, *Miner. Eng.*, 92(2016), p. 28.

[31] R.Q. Liu, W. Sun, Y.H. Hu, and D.Z. Wang, Surface chemical study of the selective separation of chalcopyrite and marmatite, *Min. Sci. Technol.*, 20(2010), No. 4, p. 542.

[32] Q.C. Feng, W.J. Zhao, S.M. Wen, and Q.B. Cao, Activation mechanism of lead ions in cassiterite flotation with salicylhydroxamic acid as collector, *Sep. Purif. Technol.*, 178(2017),p. 193.

[33] M.E. Holuszko, J.P. Franzidis, E.V. Manlapig, M.A. Hampton, B.C. Donose, and A. Nguyen, The effect of surface treatment and slime coatings on ZnS hydrophobicity, *Miner. Eng.*, 21(2008), No. 12-14, p. 958.

[34] E. Potapova, X. Yang, M. Westerstrand, M. Grahn, A. Holmgren, and J. Hedlund, Interfacial properties of natural magnetite particles compared with their synthetic analogue, *Miner. Eng.*, 36(2012), p. 187.

[35] S. Aghazadeh, S.K. Mousavinezhad, and M. Gharabaghi, Chemical and colloidal aspects of collectorless flotation behavior of sulfide and non-sulfide minerals, *Adv. colloid Interface Sci.*, 225(2015), p. 203.

[36] S. Antreich, S. Sassmann, and I. Lang, Limited accumulation of copper in heavy metal adapted mosses, *Plant Physiol. Biochem.*, 101(2016), p. 141.

[37] T. Hirajima, G.P.W. Suyantara, O. Ichikawa, A.M. Elmahdy, H. Miki, and K. Sasaki, Effect of Mg^{2+} and Ca^{2+} as divalent seawater cations on the floatability of molybdenite and chalcopyrite, *Miner. Eng.*, 96-97(2016), p. 83.

[38] P. Makreski, G. Jovanovski, B. Kaitner, A. Gajović, and T. Biljan, Minerals from Macedonia: XVIII. Vibrational spectra of some sorosilicates, *Vib. Spectrosc.*, 44(2007), No. 1, p. 162.

[39] R.L. Frost, J.M. Bouzaid, and B. Jagannadha Reddy, Vibrational spectroscopy of the sorosilicate mineral hemimorphite $Zn_4(OH)_2Si_2O_7 \cdot H_2O$, *Polyhedron*, 26(2007), No. 12, p. 2405.

[40] E.W. Giesekke, A review of spectroscopic techniques applied to the study of interactions between minerals and reagents in flotation systems, *Int. J. Miner. Process.*, 11(1983), No. 1, p. 19.

[41] P. Persson and I. Persson, Interactions between sulfide minerals and alkylxanthate ions 3. A vibration spectroscopic, calorimetric and atomic absorption spectrophotometric study of the interaction between galena and ethylxanthate ions in aqueous solution, *Colloids Surf.*, 58(1991), No.1-2, p. 161.

[42] J.O. Leppinen and J.K. Rastas, The interaction between ethyl xanthate ion and lead sulfide surface, *Colloids Surf.*, 20(1986), No. 3, p. 221.

[43] C.A. Prestidge, J. Ralston, and R.S.C. Smart, The role of cyanide in the interaction of ethyl xanthate with galena, *Colloids Surf. A*, 81(1993), p. 103.

[44] B. Liu, X.M. Wang, H. Du, J. Liu, S.L. Zheng, Y. Zhang, and J.D. Miller, The surface features of lead activation in amyl xanthate flotation of quartz, *Int. J. Miner. Process.*, 151(2016), p. 33.

[45] P. De Donato, J.M. Cases, M. Kongolo, L. Michot, and A. Burneau, Infrared investigation of amylxanthate Adsorption on galena: Influence of oxidation, pH and grinding, *Colloids Surf.*, 44(1990),p. 207.

[46] C.I. Basilio, I.J. Kartio, and R.H. Yoon, Lead activation of sphalerite during galena flotation, *Miner. Eng.*, 9(1996), No. 8, p. 869.

[47] R. Woods and G.A. Hope, Spectroelectrochemical investigations of the interaction of ethyl xanthate with copper, silver and gold: I. FT-Raman and NMR spectra of the xanthate compounds, *Colloids Surf. A*, 137(1998), No. 1-3, p. 319.

[48] P. Hellström, S. Öberg, A. Fredriksson, and A. Holmgren, A theoretical and experimental study of vibrational properties of alkyl xanthates, *Spectrochim. Acta Part A*, 65(2006), No. 3-4, p. 887.

[49] P. Sharma, K.H. Rao, K.S.E. Forssberg, and K. Natarajan, Surface chemical characterisation of Paenibacillus polymyxa before and after adaptation to sulfide minerals, *Int. J. Miner. Process.*, 62(2001), No. 1-4, p. 3.

[50] K.P. Wang, L. Wang, M.L. Cao, and Q. Liu, Xanthation-modified polyacrylamide and spectroscopic investigation

of its adsorption onto mineral surfaces, *Miner. Eng.*, 39(2012), p. 1.

[51] S.A. Markgraf and A.S. Bhalla, Pyroelectric and dielectric properties of hemimorphite, $Zn_2Si_2O_7(OH)_2 \cdot H_2O$, *Mater. Lett.*, 8(1989), No. 5, p. 179.

[52] L. Chung-Cherng and S. Pouyan, Role of screw axes in dissolution of willemite, *Geochim. Cosmochim. Acta*, 57(1993), No. 8, p. 1649.

[53] P.L. Houston, *Chemical Kinetics and Reaction Dynamics*, Springer Netherlands, Berlin, Germany, 2006, p. 407.

[54] D. Fornasiero and J. Ralston, Effect of surface oxide/hydroxide products on the collectorless flotation of copper-activated sphalerite, *Int. J. Miner. Process.*, 78(2006), No. 4, p. 231.

[55] J.Q. Jin, J.D. Miller, L.X. Dang, and C.D. Wick, Effect of Cu^{2+} activation on interfacial water structure at the sphalerite surface as studied by molecular dynamics simulation, *Int. J. Miner. Process.*, 145(2015), p. 66.

[56] T. Khmeleva, W. Skinner, and D. Beattie, Depressing mechanisms of sodium bisulphite in the collectorless flotation of copper-activated sphalerite, *Int. J. Miner. Process.*, 76(2005), No. 1-2, p. 43.

[57] Z. Chen and R.H. Yoon, Electrochemistry of copper activation of sphalerite at pH 9.2, *Int. J. Miner. Process.*, 58(2000), No. 1-4, p. 57.

[58] T. Albrecht, J. Addai-Mensah, and D. Fornasiero, Critical copper concentration in sphalerite flotation: Effect of temperature and collector, *Int. J. Miner. Process.*, 146(2016), p. 15.

[59] F. Rashchi, C. Sui, and J.A. Finch, Sphalerite activation and surface Pb ion concentration, *Int. J. Miner. Process.*, 67(2002), No. 1-4, p. 43.

[60] J. Laskowski, Q. Liu, and Y. Zhan, Sphalerite activation: Flotation and electrokinetic studies, *Miner. Eng.*, 10(1997), No. 8, p. 787.